International Journal of Research in Advent Technology, Vol.6, No.7, July 2018
E-ISSN: 2321-9637
Available online at www.ijrat.org

Unsteady MHD Boundary Layer Heat and Mass Transfer Flow of Micropolar Fluid over Porous Stretching Sheet with Soret and Dufour Effects

S.R. Ravichandra Babu[1,*], S. Venkateswarlu[2], K. Jaya Lakshmi[3]
[1, *]*Research scholar, JNTUA, Anantapuramu, A.P, India.*
[2]*Department of mathematics, RGM College of Engineering & Technology, Nandyala, A.P, India.*
[3]*Department of mathematics, Jawaharlal Nehru Technological University, Anantapur, Anantapuram, A.P, India.*
Corresponding author Email: ***ravichandrababusr@gmail.com.***

Abstract- The impact of Soret and Dufour effects on unsteady MHD boundary layer flow, heat and mass transfer analysis over a stretching sheet embedded in porous media filled with viscous micropolar fluid is numerically investigated. Suitable similarity variables reduced the PDEs in to ODEs and are solved by using FEM. The sway of various parameters on velocity, micro-rotation, temperature and concentration profiles is portrayed graphically. Furthermore, the values of skin-friction coefficient, couple stress coefficient, rates of heat and mass transfer are also calculated.

1. INTRODUCTION

Micropolar fluid flow through porous media is one of leading area of research, because of its numerous applications in brain flow, exotic lubricants, liquid crystals, blood flow in animals, etc. keeping above applications in mind, Chamkha et al. [1] perceived the impact of radiation and chemical reaction on unsteady MHD micropolar fluid past a heated vertical plate. Rashidi et al. [2] have presented the sway of radiation on flow of micropolar fluid saturated in porous media and Homotopy analysis method (HAM) is used to obtain accurate and analytical solution. Shadloo et al. [3] discussed the heat transfer flow of micropolar fluid over stretching sheet embedded in porous media with thermal radiation. They found that as the values of microrotation parameter increases the velocity of the fluid worsens, whereas, angular velocity upsurges.

The problem of two dimensional boundary layer flow, heat and mass transfer over a continuous stretching heated surface through porous medium finds numerous and wide range of applications in many engineering and manufacturing disciplines such as glass blowing, extrusion process, melt-spinning, food-stuff processing, design of heat exchangers, wire and fiber coating, glass-fiber production, manufacture of plastic and rubber sheets, cooling of a large metallic plate in a bath and continuous casting. Yacob et al. [4] discussed stagnation-point flow of micropolar fluid over a stretching/shrinking sheet. Mahmood et al. [5] studied heat transfer characteristics of stagnation point flow of micropolar second grade fluid over a stretching sheet. Pal et al. [6] deliberated the impact of non – uniform heat source/sink on Darcy–Forchheimer convective flow of micro – polar fluid over stretching sheet with radiation.

Soret and Dufour effects are very significant for the fluids which have higher temperature and concentration gradients and its applications can be found in the area of reactor safety, combustion flames and solar collectors as well as building energy conservation. In view of above applications several others [7, 8, 9, 10, 11] have discussed the impact of magnetic field, Soret and Dufour effects on boundary layer heat and mass transfer flow over different geometries.

2. MATHEMATICAL ANALYSIS

We consider two-dimensional, unsteady, viscous, electrically conducting, heat and mass transfer of micropolar fluid over porous stretching sheet as shown in Fig. 1. A uniform transverse magnetic field (B_0) is applied along the y-axis. T_w and C_w are uniform temperature and concentration at surface and are assumed to be greater than the ambient temperature and

concentration T_∞ and C_∞ respectively Under the reference works of Mohanty et al. [12], the governing boundary-layer equations take the form:

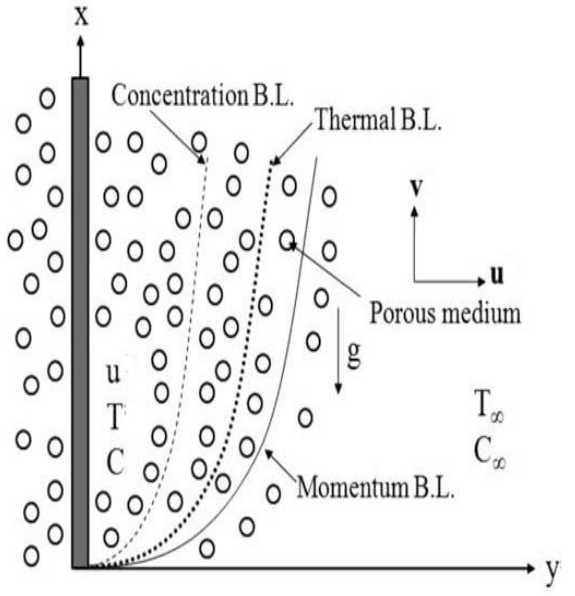

Fig. 1. Physical model and coordinate system.

$$\frac{\partial u}{\partial x}+\frac{\partial v}{\partial y}=0 \tag{1}$$

$$\frac{\partial u}{\partial t}+u\frac{\partial u}{\partial x}+v\frac{\partial u}{\partial y}=\left(\frac{\mu+\kappa}{\rho}\right)\frac{\partial^2 u}{\partial y^2}+\left(\frac{\kappa}{\rho}\right)\frac{\partial W}{\partial y} + g_a[\beta(T-T_\infty)+\beta'(C-C_\infty)]-\frac{\mu}{\rho\kappa}u-\frac{\sigma B_0^2}{\rho}u \tag{2}$$

$$\frac{\partial W}{\partial t}+u\frac{\partial W}{\partial x}+v\frac{\partial W}{\partial y}=-\frac{\kappa}{\rho J}\left(2W+\frac{\partial u}{\partial y}\right)+\frac{\gamma}{\rho J}\frac{\partial^2 W}{\partial y^2} \tag{3}$$

$$\frac{\partial T}{\partial t}+u\frac{\partial T}{\partial x}+v\frac{\partial T}{\partial y}=\alpha\frac{\partial^2 T}{\partial y^2}+\frac{\nu}{c_p}\left(\frac{\partial u}{\partial y}\right)^2+\frac{D_m k_T}{c_s c_p}\frac{\partial^2 C}{\partial y^2} \tag{4}$$

$$\frac{\partial C}{\partial t}+u\frac{\partial C}{\partial x}+v\frac{\partial C}{\partial y}=D_m\frac{\partial^2 C}{\partial y^2}+\frac{D_m k_T}{T_m}\frac{\partial^2 T}{\partial y^2} \tag{5}$$

The associated boundary conditions on the vertical surface are defined as follows,

$$\begin{aligned} u=U_w(x)=ax, v=V_1(x), T=T_w,\\ C=C_w, W=0,\ at\ y=0.\\ u\to 0, W\to 0,\ T\to T_\infty,\ C\to C_\infty,\ at\ y\to\infty. \end{aligned} \tag{6}$$

The term $V_1=-\sqrt{\frac{\nu a}{2}}V_0$ represents the mass transfer at the surface with $V_1<0$ for suction and $V_1>0$ for injection.

We now introduced similarity variables as

$$\eta=\sqrt{\frac{a}{\nu(1-ct)}}\,y,\ \psi=\sqrt{\frac{\nu a}{1-ct}}\,f,\ u=\frac{ax}{1-ct}f'$$

$$v=-\sqrt{\frac{\nu a}{1-ct}}\,f,\ W=\sqrt{\frac{a^3}{\nu(1-ct)^3}}\,x\,g$$

$$T=T_\infty+\frac{bx}{(1-ct)^2}\theta,\ C=C_\infty+\frac{dx}{(1-ct)^2}\phi. \tag{7}$$

Using eqn. (7), the governing equations (2) – (5) are transformed into the following form

$$(1+A1)f'''+ff''-f'^2-A\left(f'+\frac{1}{2}\eta f''\right)+ A1g'+\ g_r\theta+g_m\phi-(M+K)f'=0 \tag{8}$$

$$\lambda g''+fg'-gf'-\frac{A}{2}(3g+\eta g')+ A1\,B(2g+f'')=0 \tag{9}$$

$$\theta''+Pr(f\theta'-f'\theta)-Pr\,\frac{A}{2}(4\theta+\eta\theta')+ Ec\,(f'')^2+Du\,\phi''=0 \tag{10}$$

$$\phi''-Sc\,(f'\phi-f\phi')-Sc\,\frac{A}{2}(4\phi+\eta\phi')+ Sc\,Sr\,\theta''=0 \tag{11}$$

The corresponding transformed boundary conditions are

$$f'=1,\ f=V_0,\ g=0,\ \theta=1,\ \phi=1,\ \text{at}\quad y=0$$

$$f'=0,\quad g=0,\quad \theta=0,\quad \phi=0\quad \text{at}\quad y\to\infty \tag{12}$$

Where $A1=\frac{\kappa}{\mu}$, $g_r=\frac{g_a\beta b}{a^2}$, $g_m=\frac{g_a\beta' l}{a^2}$, $A=\frac{c}{a}$ $K=\frac{\nu(1-ct)}{k\,a}$, $Pr=\frac{\nu}{\alpha}$, $\lambda_0=\frac{\nu}{\mu\,j}$, $Sc=\frac{\nu}{D_m}$

$B=\frac{\nu\,(1-ct)}{j\,a}$, $Du=\frac{D_m k_T\,l}{c_s c_p b\,\nu}$, $Sr=\frac{D_m k_T}{\nu T_m}$,

$Ec=\frac{a^2 x}{c_p\,b}$ $M=\frac{\sigma B_0^2(1-ct)}{\rho\,a}$.

The skin friction coefficient(C_{fx}), couple stress coefficient(C_{sx}), Nusselt number (Nu_x) and Sherwood number (Sh_x) are defined as

$$C_{fx}=\frac{2(1+A1)\,f''(0)}{Re_x^{\frac{1}{2}}},\ C_{sx}=\frac{\nu\,a\,U_w h'(0)}{Re_x^{\frac{1}{2}}}$$

$$Nu_x=-\frac{\theta'(0)}{Re_x^{\frac{1}{2}}},\quad Sh_x=-\frac{\phi'(0)}{Re_x^{\frac{1}{2}}}.$$

The eqns. (8) – (11) are solved using Finite-element method [13, 14, 15, 16].

3. RESULTS AND DISCUSSION

The distributions of velocity, temperature and concentration are presented in Figs. 2 – 16. The Comparison of present results with the results reported by Mohanty et al. [12] is made and found good agreement which is shown in Table 1. It is observed from Fig.2 that the velocity of the fluid decreases with increase in the value of the suction parameter ($V_0 > 0$). The micro-rotation profiles also decelerates with increasing values of ($V_0 > 0$) (Fig.3). It is seen observed from Fig.4 that temperature profiles decreases with increase in the values of ($V_0 > 0$). Furthermore, the concentration profiles also diminishes in the boundary layer regime with increase in the values of ($V_0 > 0$) and is shown in Fig.5. It is noticed from Figs. 6 &7 that both velocity distributions depreciate with rising values of (*M*). The temperature and concentration of the fluid elevates with higher values of M and is shown in Figs. 8 & 9. The profiles of velocity are the decreasing functions of unsteadiness parameter (τ) in the boundary layer regime (Fig. 10). It can be seen that temperature profiles decelerates with increase in the values of unsteadiness parameter (α) as shown in Fig. 11. Furthermore, the concentration profiles also decreases in the flow region and is shown in Fig. 12. Figure 13 depicts the effect of Eckert number (*Ec*) on temperature profiles in the boundary layer regime. The thickness of thermal boundary layer is boosted in the flow region as the values of Eckert number (*Ec*) rises. The impact of Soret effect (*Sr*) on concentration profiles is portrayed in Figs. 14. It is clearly observed that concentration profiles increases at all points in the flow field with the increasing values of Soret number (*Sr*). The impact of Dufour number (*Du*) on temperature profiles is portrayed in Fig. 15. The temperature of the fluid raises in the boundary layer regime as the (*Du*) increases. It is worth to mention that velocity profiles (Figs. 16) heighten in the fluid regime with the increasing values of (*A1*).

It is seen from Table 2 that the values of local skin-friction co-efficient, Nusselt number and sherwood numbers are depreciates, whereas, the values of couple stress coefficient elevates with increase in the values of (*M*). It is clear from this table that the values of skin-friction coefficient worsens, however, the couple stress coefficient, dimensionless heat and mass transfer rates are boosted with the higher values of suction parameter ($V_0 > 0$). It is clear from this table that the values of skin-friction coefficient, Nusselt and Sherwood number are increased, whereas, the values of micro-rotation diminishes with the higher values of (τ). It is noticed that the values of $\left(f''(0)\right)$, $\left(g'(0)\right)$ and $\left(-\phi'(0)\right)$ decreases, whereas, $\left(-\theta'(0)\right)$ values hightens as the values of (*Sr*) rises. The dimensionless velocity, micro-rotation and heat transfer rates are decreased, whereas, the dimensionless mass transfer rates increases with the increasing values of (*Du*). The values of all non-dimensional parameters, skin-friction co-efficient, couple stress coefficient, local Nusselt number and Sherwood number upsurges as the values of micro-rotation parameter (*A1*) increases.

4. CONCLUSION

The combined influence of Thermo – diffusion and Diffusion – thermo effect on unsteady MHD boundary layer flow, heat and mass transfer characteristics of viscous micropolar fluid over a stretching sheet by taking suction/injection into the account is studied numerically in this paper. Suction parameter ($V_0 > 0$) deteriorates the velocity, angular velocity, temperature and concentration of the fluid in the boundary layer regime. The velocity of the fluid diminishes, whereas, temperature of the fluid heightens with rising values of (*M*). Soret effect enhances the concentration profiles, whereas, depreciates the temperature profiles. However, exact reverse trend is noticed in the profiles with higher values of (*Du*).

GRAPHS

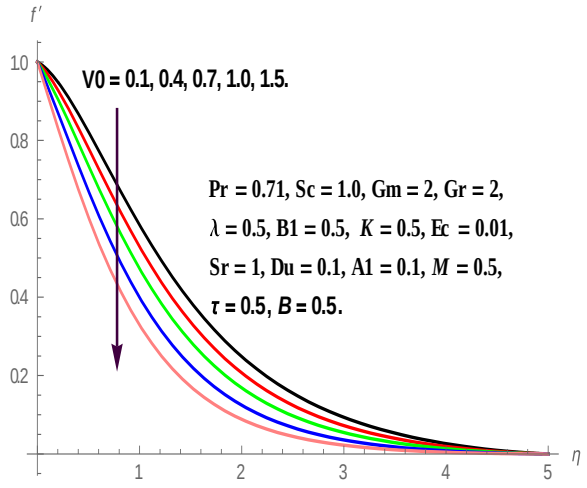

Fig. 2. Effect of (V_0) on Velocity profiles.

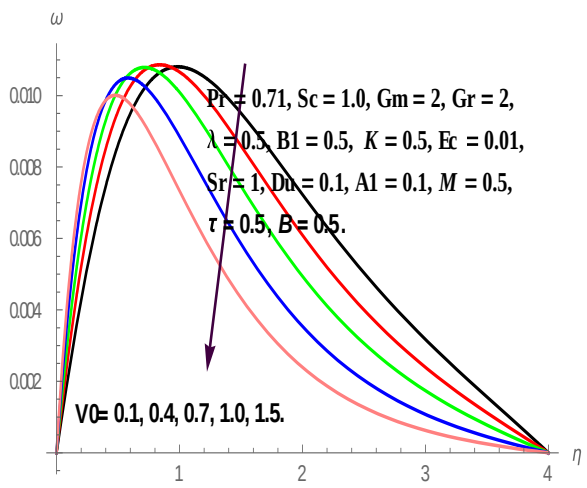

Fig. 3. Effect of (V_0) on angular velocity profiles.

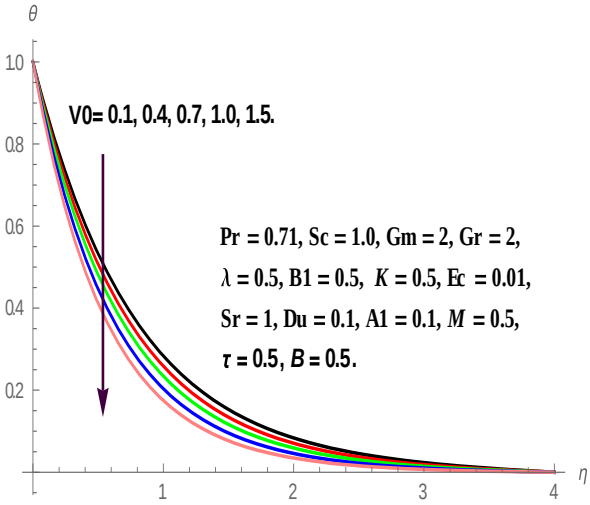

Fig. 4. Effect of (V_0) on Temperature profiles.

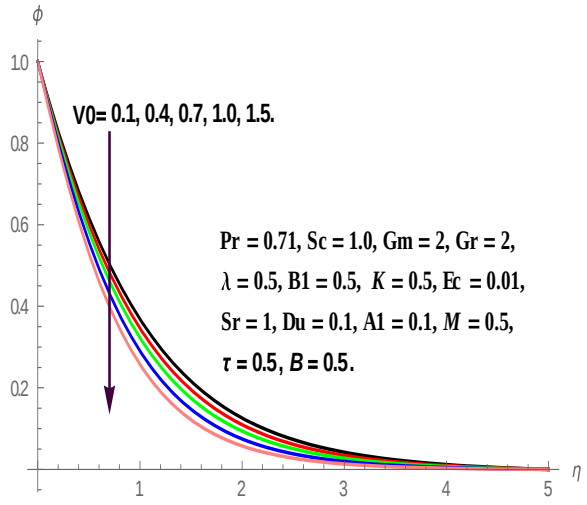

Fig. 5. Effect of (V_0) on Concentration profiles.

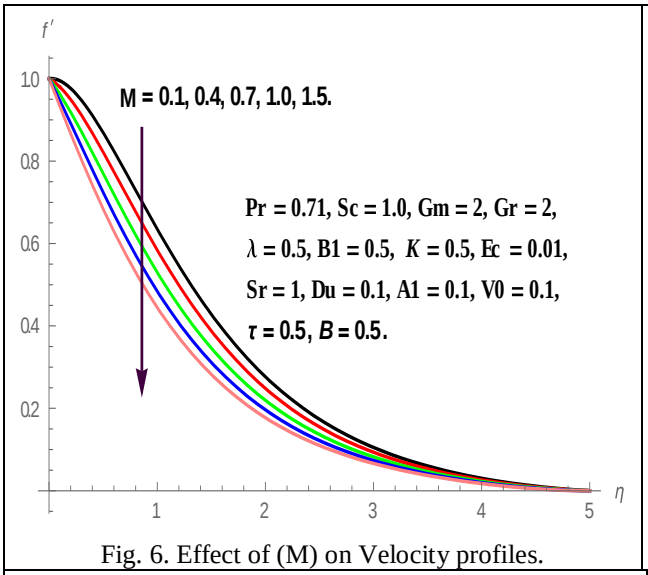

Fig. 6. Effect of (M) on Velocity profiles.

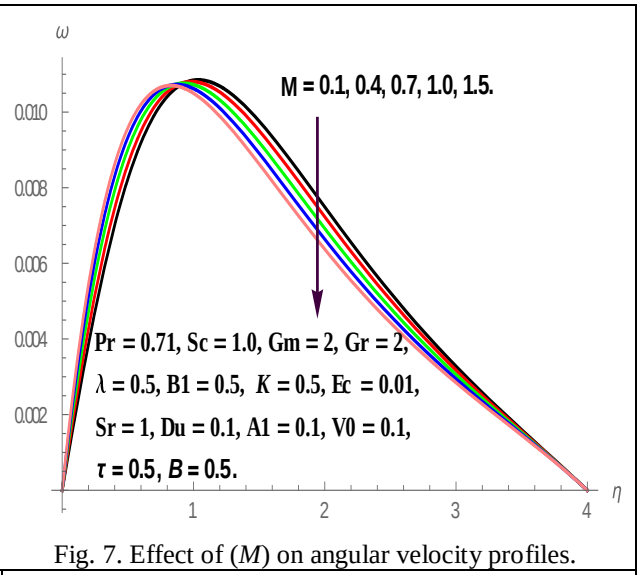

Fig. 7. Effect of (*M*) on angular velocity profiles.

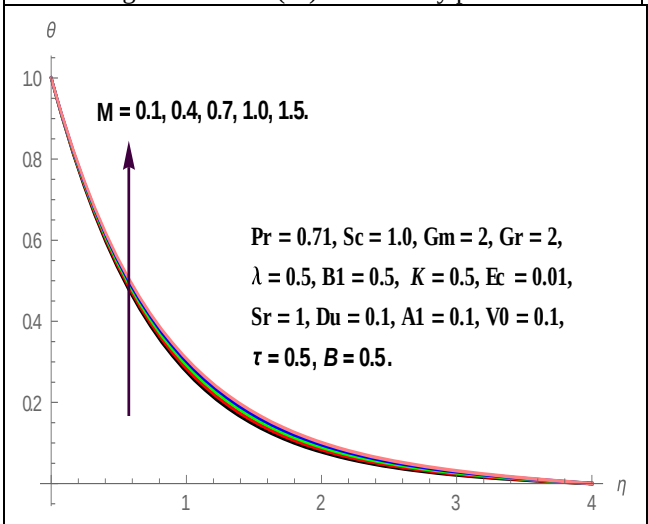

Fig. 8. Effect of (*M*) on Temperature profiles.

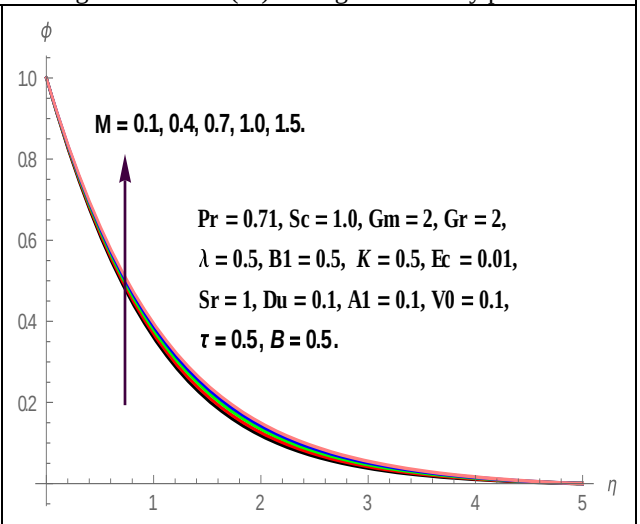

Fig. 9. Effect of (*M*) on Concentration profiles.

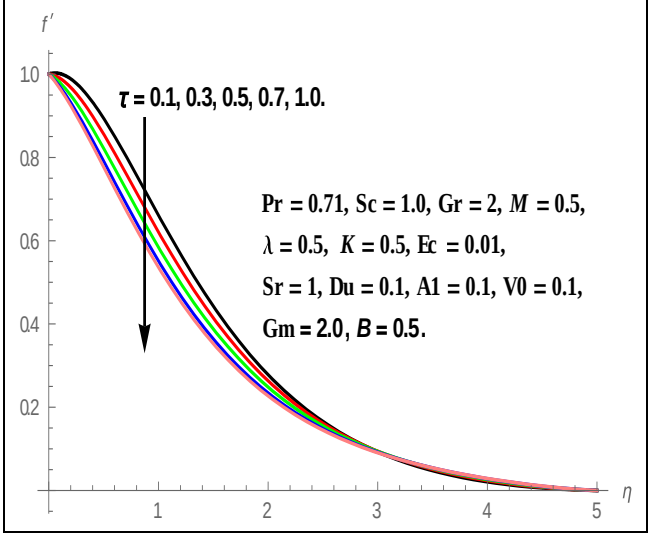

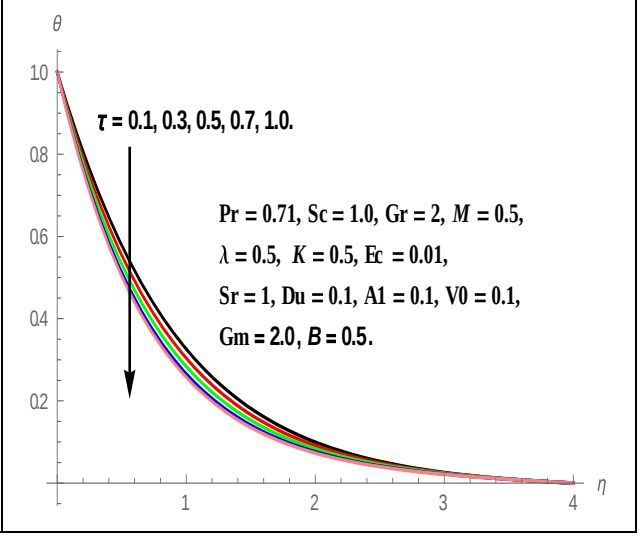

Fig. 10. Effect of (τ) on Velocity profiles.

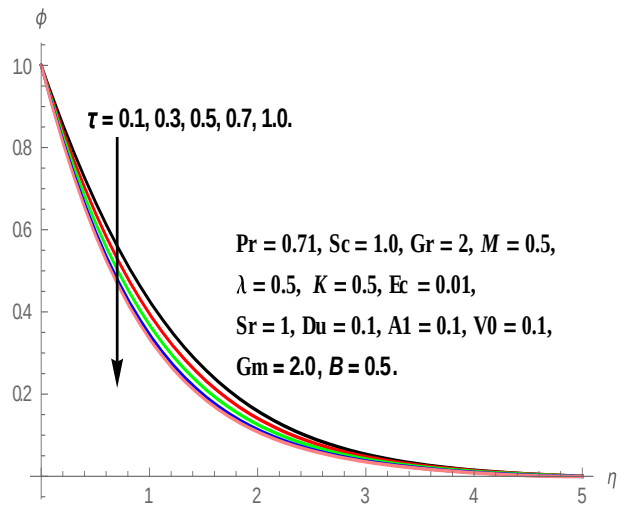

Fig. 11. Effect of (τ) on Temperature profiles.

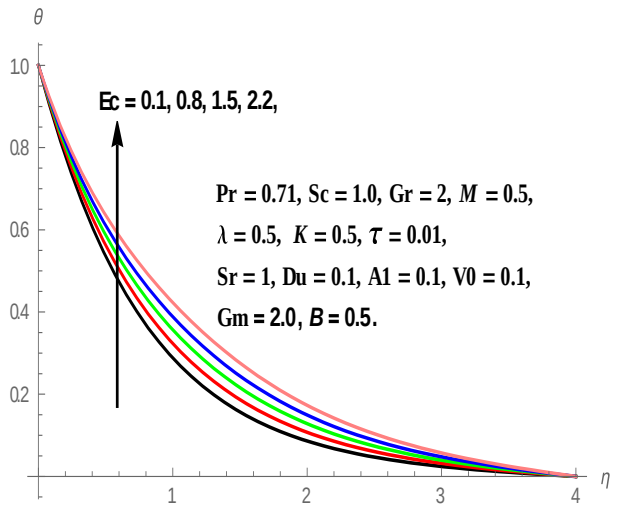

Fig. 12. Effect of (τ) on Concentration profiles.

Fig. 13. Effect of (*Ec*) on Temperature profiles.

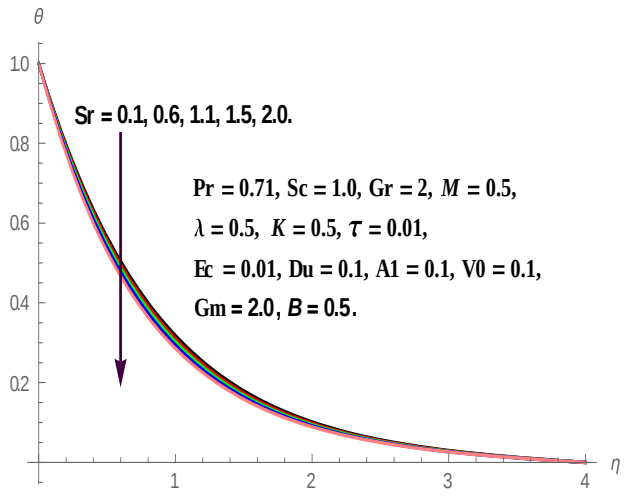

Fig. 14. Effect of (*Sr*) on Temperature profiles.

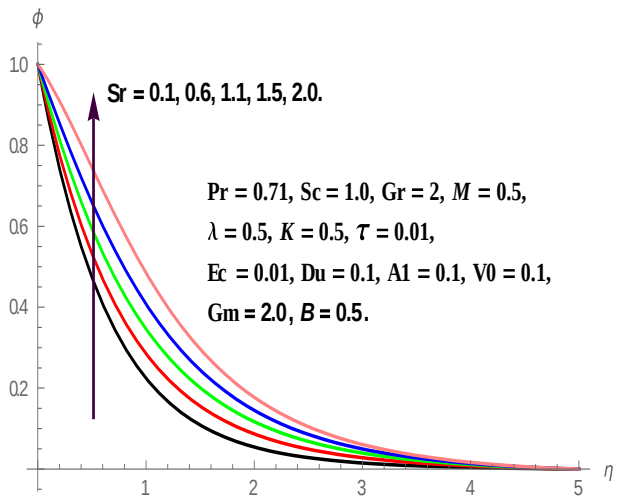

Fig. 15. Effect of (*Sr*) on Concentration profiles.

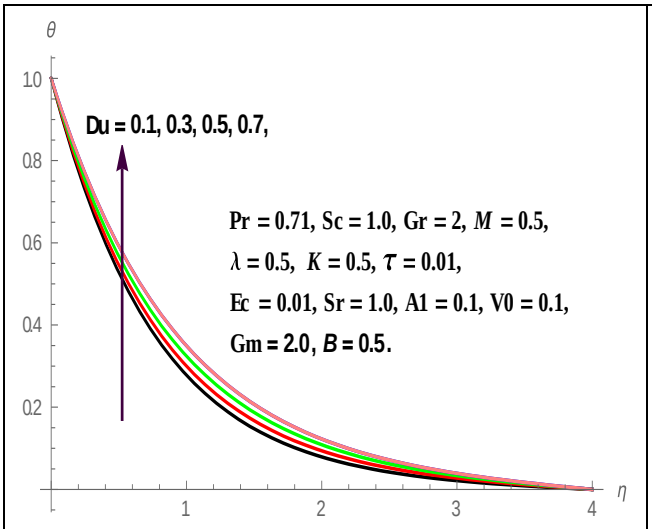

Fig. 16. Effect of (*Du*) on Temperature profiles.

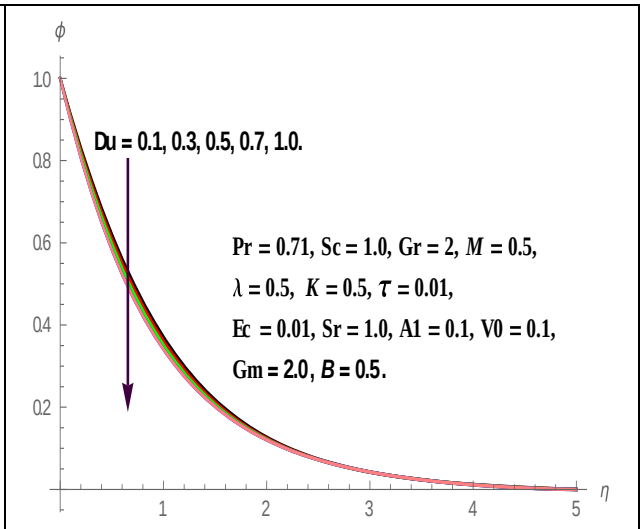

Fig. 17. Effect of (*Du*) on Concentration profiles.

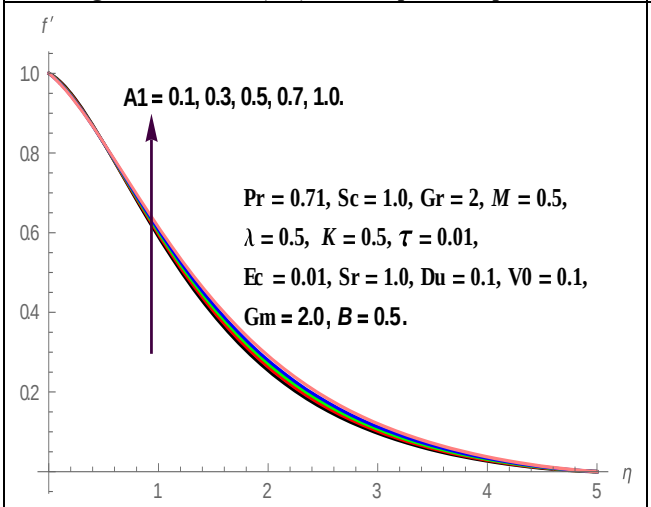

Fig. 18. Effect of (*A1*) on Velocity profiles.

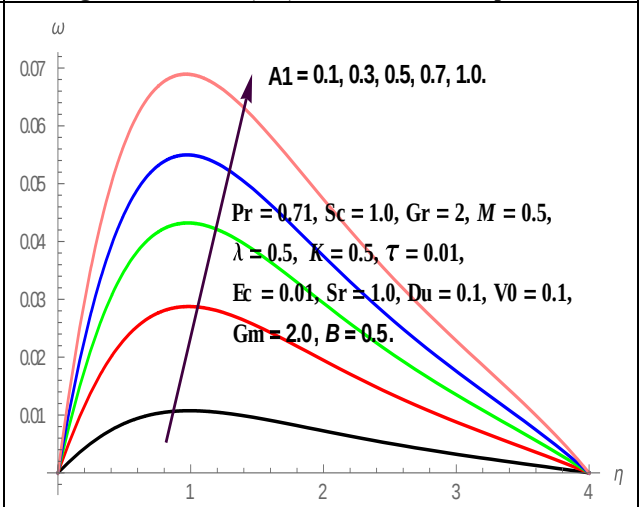

Fig. 19. Effect of (*A1*) on angular velocity profiles.

Table 1: Comparison of present results with Mohanty et al. [12].

Parameter							*Cf*		*Nux*		*Shx*	
Gr	*Gc*	*Pr*	*Sc*	*M*	*K*	*Ec*	*Mohanty et al.* [12]	*Present Study*	*Mohanty et al.* [12]	*Present S*	*Mohanty et al.* [12]	*Present*
0.0	0.0	0.72	0.00	0	100	0.00	−0.81861	−0.81873	0.85604	0.85619	0.16666	0.16671
0.1	0.0	0.72	0.00	0	100	0.00	−0.78025	−0.78019	0.86514	0.86526	0.42252	0.42263
0.1	0.0	0.72	0.22	0	100	0.00	−0.78025	−0.78019	0.86514	0.86526	0.42252	0.42263
0.1	0.0	0.72	0.22	1	100	0.00	−1.11781	−1.11776	0.78477	0.78482	0.37866	0.37872
0.1	0.0	0.72	0.22	1	0.5	0.01	−1.59782	−1.59773	0.68391	0.68386	0.33393	0.33385
0.1	0.0	0.72	0.22	1	100	0.01	−1.11775	−1.11766	0.77999	0.77981	0.37867	0.37874
0.1	0.0	0.72	0.22	1	0.5	0.01	−1.59777	−1.59782	0.67651	0.67646	0.33394	0.33398
0.1	0.1	7.00	0.22	1	100	0.01	−1.09307	−1.09311	3.02046	3.02052	0.38361	0.38370

0.5	0.1	0.72	0.22	1	100	0.01	−0.93986	−0.93991	0.82922	0.82931	0.40495	0.40486
0.1	0.1	0.72	0.22	1	100	0.01	−1.06792	−1.06798	0.79858	0.79863	0.38891	0.38896
0.5	0.1	0.72	0.22	1	0.5	0.01	−1.44651	−1.44667	0.72576	0.72569	0.35583	0.35591

Table 2: Influence of various parameters on Skin-friction co-efficient $(f''(0))$, Couple stress coefficient $(h'(0))$, local Nusselt number $(-\theta'(0))$ and local Sherwood number $(-\phi'(0))$.

M	V_0	τ	Sr	Du	$A1$	C_{fx}	C_{sx}	Nu_x	Sh_x
0.1	0.5	0.5	1.0	0.1	0.1	−0.029503	0.020189	1.263071	0.930092
0.4	0.5	0.5	1.0	0.1	0.1	−0.140078	0.023735	1.247951	0.916867
0.7	0.5	0.5	1.0	0.1	0.1	−0.334706	0.027632	1.230871	0.902205
1.0	0.5	0.5	1.0	0.1	0.1	−0.513352	0.031039	1.215510	0.889266
1.5	0.5	0.5	1.0	0.1	0.1	−0.678789	0.034055	1.201602	0.877778
0.5	0.1	0.5	1.0	0.1	0.1	−0.140078	0.023735	1.247951	0.916867
0.5	0.4	0.5	1.0	0.1	0.1	−0.250201	0.031057	1.352539	0.955381
0.5	0.7	0.5	1.0	0.1	0.1	−0.380552	0.038807	1.464718	0.994421
0.5	1.0	0.5	1.0	0.1	0.1	−0.587237	0.049129	1.626014	1.048395
0.5	1.5	0.5	1.0	0.1	0.1	−0.831464	0.058702	1.800411	1.106039
0.5	0.5	0.1	1.0	0.1	0.1	0.095679	0.025293	1.054316	0.758771
0.5	0.5	0.3	1.0	0.1	0.1	0.126948	0.024305	1.154059	0.841319
0.5	0.5	0.5	1.0	0.1	0.1	0.140078	0.023735	1.247951	0.916867
0.5	0.5	0.7	1.0	0.1	0.1	0.244878	0.023491	1.336645	0.987009
0.5	0.5	1.0	1.0	0.1	0.1	0.294497	0.023461	1.379229	1.020413
0.5	0.5	0.5	0.1	0.1	0.1	0.232941	0.026897	1.131447	1.473229
0.5	0.5	0.5	0.6	0.1	0.1	0.189636	0.025347	1.164016	1.250944
0.5	0.5	0.5	1.1	0.1	0.1	0.145116	0.023823	1.198808	1.008882
0.5	0.5	0.5	1.5	0.1	0.1	0.099296	0.022319	1.236250	0.743977
0.5	0.5	0.5	2.0	0.1	0.1	0.039967	0.020474	1.287598	0.374770
0.5	0.5	0.5	1.0	0.1	0.1	0.142382	0.023843	1.265463	0.903797
0.5	0.5	0.5	1.0	0.3	0.1	0.133788	0.023442	1.207902	0.944932
0.5	0.5	0.5	1.0	0.5	0.1	0.124237	0.023009	1.135199	0.998566
0.5	0.5	0.5	1.0	0.7	0.1	0.114095	0.022566	1.043630	1.068728
0.5	0.5	0.5	1.0	1.0	0.1	0.110503	0.022566	1.043630	1.068728
0.5	0.5	0.5	1.0	0.1	0.1	0.133788	0.023442	1.207902	0.944932
0.5	0.5	0.5	1.0	0.1	0.3	0.163289	0.065066	1.208374	0.945285
0.5	0.5	0.5	1.0	0.1	0.5	0.185200	0.101119	1.208910	0.945701
0.5	0.5	0.5	1.0	0.1	0.7	0.201958	0.132848	1.209486	0.946153
0.5	0.5	0.5	1.0	0.1	1.0	0.220553	0.174194	1.210388	0.946864

REFERENCES

[1]. Chamkha, A. J. Mohammad, R.A. and Ahmad, E., Meccanica, vo. **46**, pp. 399 – 411, 2011.

[2]. Rashidi, M.M. Mohimanian pour, S.A. and Abbasbandy, S., Commun. Nonlinear Sci. Numer. Simul., vol. **16**, pp. 1874–1889, 2011.

[3]. Shadloo, M.S. Kimiaeifar, A. and Bagheri D., Int. J. Numer. Meth. Heat Fluid Flow vol. **23**, pp. 289–304, 2013.

[4]. Yacob, N.A. Ishak, A. and Pop. I., Comput.Fluids vol. **47**, pp. 16–21, 2011.

[5]. Mahmood, R. Nadeem, S. and Akber, N.S., J. Taiwan Inst. Chem. Eng.,vol. **44**, pp. 586–595, 2013.

[6]. Pal, D. and Chatterjee, S., J. Appl. Fluid Mech., vol. **8**, 207–212, 2015.

[7]. Dulal Pal. and Mondal, H., International communications in heat and mass transfer, vol. **38**, pp. 463-467, 2011.

[8]. Makinde, O.D., Latin American Applied Research vol. **41**, pp. 63-68, 2011.

[9]. Reddy, P.S. and Rao, V.P., Journal of Applied Fluid Mechanics, vol. **5(4)**, pp. 139-144, 2012.

[10]. Chamkha, A.J. and Rashad, A.M., The Canadian Journal of Chemical Engineering, DOI 10.1002/cjce.21894, 2014.

[11]. Sudarsana Reddy, P. and Chamkha, A.J., Advanced Powder Technology vol. **27**, pp. 1207-1218, (2016).

[12]. Mohanty, B. Mishra, S.R. and Pattanayak, H.B, Alexandria Engineering Journal vol. **54**, pp. 223–232, 2015.

[13]. Anwar Bég, O. Takhar, H.S. Bhargava, R. Rawat, S. and Prasad, V.R., Phys. Scr., vol. **77**, pp. 1–11, 2008.

[14]. Sudarsana Reddy, P. and Chamkha, A.J., Journal of Naval Architecture and Marine Engineering vol. **13**, pp.39-50, (2016).

[15]. Sudarsana Reddy, P. and Chamkha, A.J, Journal of Applied Fluid Mechanics vol. **9**, pp. 2443-2455, (2016).

[16]. Rana, P. and Bhargava, R., Comm. Nonlinear Sci. Numer. Simulat., vol. **17**, pp. 212 – 226, 2012.